Thermal fluctuations in ultrasmall intrinsic Josephson junctions

A. Franz, Y. Koval, D. Vasyukov, and P. Müller
Physikalisches Institut III, Universität Erlangen-Nürnberg, D-91058 Erlangen, Germany

H. Schneidewind
Institut für Physikalische Hochtechnologie, P.O. Box 100239, D-07702 Jena, Germany

D.A. Ryndyk* and J. Keller
Institut für Theoretische Physik, Universität Regensburg, D-93040 Regensburg, Germany

C. Helm
Institut für Theoretische Physik, ETH Zürich, CH-8093 Zürich, Switzerland
(Dated: 9th June 2003)

Current-voltage curves of small area hysteretic intrinsic Josephson junctions, for which the Josephson energy $E_J = \hbar J_c/2e$ is of order of thermal energy kT, are investigated. A non-monotonic temperature dependence of the switching current is observed and explained by thermal phase fluctuations. At low temperatures premature switching from the superconducting into the resistive state is the most important effect of fluctuations. At high temperatures only a single resistive branch is observed. At the cross-over temperature a hysteretic phase-diffusion branch exists. It shows the importance of a frequency-dependent impedance of an external circuit formed by the leads.

PACS numbers: 74.40.+k, 74.50.+r

I. INTRODUCTION

In the strongly anisotropic cuprate superconductors, such as $Bi_2Sr_2CaCu_2O_{8+\delta}$ (BSCCO) or $Tl_2Ba_2CaCu_2O_{8+\delta}$ (TBCCO), the CuO_2 layers together with the intermediate material form a stack of Josephson junctions. In the presence of a bias current perpendicular to the layers each junction of the stack is either in the resistive or in the superconducting state leading to the well-known multibranch structure of the IV-curves, see Ref. 1,2,3,4 and references therein.

The effect of thermal noise on the properties of Josephson junctions made from *low-temperature* superconductors, and in particular on the critical current and voltage-current curves, has been investigated experimentally and theoretically in many publications, see Ref. 5,6,7,8. For *high-temperature* superconductors considerable interest has been attracted to the problems of thermal fluctuations in the vortex state, see Ref. 9,10,11,12,13, but, to our knowledge, no detailed study of the influence of thermal fluctuations on the critical current and current-voltage curves of mesoscopic intrinsic Josephson junctions has been carried out. Some fluctuation effects are reported recently in Ref. 14.

In our paper we present the results of experimental and theoretical investigations of small area intrinsic Josephson junctions, when the Josephson energy $E_J(T) = J_c(T)/2e$ is of the order of kT (k is the Boltzmann constant). For temperatures $T \geq T^*$ thermal fluctuations become important. This cross-over temperature can be estimated with help of Fig. 1, where the Ambegaokar-Baratoff temperature dependence of the critical current density $j_c(T)$ is plotted together with the linear functions $2ekT/\hbar A$ (marked as $kT = E_J$ in the figure) for mesas with different area A. T^* can be read-off from the crossing points of the curves.

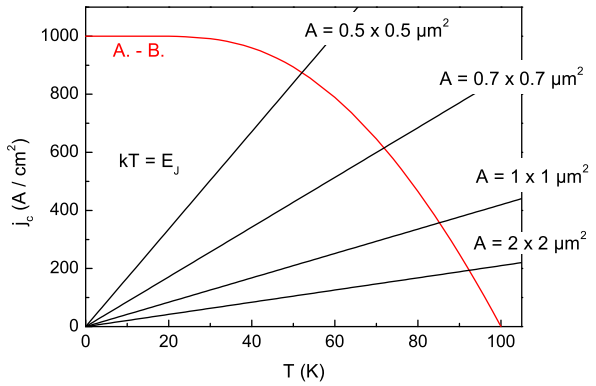

Figure 1: Estimation of crossover temperature T^* from the condition $E_J(T^*) \approx kT^*$ for mesas of different area.

We discuss in the following junctions with cross-over temperatures in the range of 10-60 K ($A \sim 0.5 \times 0.5\,\mu$m). Note that for all our samples the charging energy $E_c = e^2/2C$ is still small compared to E_J, such that quantum effects (Coulomb blockade and quantum tunneling) are not essential. From the behaviour of the current-voltage characteristics of the junctions three temperature regimes can be distinguished. At low temperatures, $T < T^*$, straight lines with hysteretic jumps

*On leave from the Institute for Physics of Microstructures, RAS, Nizhny Novgorod, Russia

to other resistive branches are observed (see Fig. 3 and Fig. 8). At temperature $T \sim T^*$ the current voltage curves are bended near the critical current (like in Fig. 4 and Fig. 11), but still some hysteresis is found. At high temperatures, $T > T^*$, no more jumps in the current voltage curve occur and no real critical current exists, but still a maximum in the curvature can be distinguished (see Fig. 5), which can be regarded as maximum of the supercurrent. In order to describe all temperature regimes together we introduce the concept of a "switching" current, which will be defined below. It replaces the critical current in the non-hysteretic high-temperature regime. A plot of the switching current as function of temperature shows a rather non-monotonic behaviour, which is very different from the AB-curve found for the critical current of large junctions. We will show below that the temperature dependence of the switching current, in particular the sharp drop, can be explained by phase diffusion processes. This will be done with help of an extended RSJ model containing thermal current noise and the coupling to an external RC circuit (Fig. 2). The latter is necessary to obtain the observed hysteretic behaviour for the phase diffusion branch at intermediate temperatures $T \sim T^*$. In our case the external RC circuit is formed most probably by a large capacitance between the ground superconducting layer and the upper electrode together with the resistance of the contact between mesa and upper electrode.

The paper is organized as follows. In section II we discuss typical voltage-current curves at different temperatures and give a brief summary of the theory used in calculations. In section III sample preparation and experimental set-up are described. The main section IV is devoted to experimental results and their discussion. Here also a discussion of magnetic field effects is included.

II. OUTLINE OF THE THEORY

A. RSJ + Johnson noise

The simplest model to describe thermal phase fluctuations in Josephson systems is the usual RSJ model with Johnson noise

$$\frac{\hbar C}{2e}\frac{d^2\varphi}{dt^2} + \frac{\hbar}{2eR}\frac{d\varphi}{dt} + J_c \sin\varphi = J + J_T, \qquad (1)$$

$$\langle J_T(t) J_T(t')\rangle = \frac{2kT}{R}\delta(t-t'). \qquad (2)$$

Here φ is the Josephson phase difference, C, $R(T)$, $J_c(T)$ are junction capacitance, resistance, and critical current, J is the bias current, $J_T(t)$ is a random current noise. This equation can be written in dimensionless form as

$$\beta\frac{d^2\varphi}{d\tau^2} + \frac{d\varphi}{d\tau} + \sin\varphi = j + j_T, \qquad (3)$$

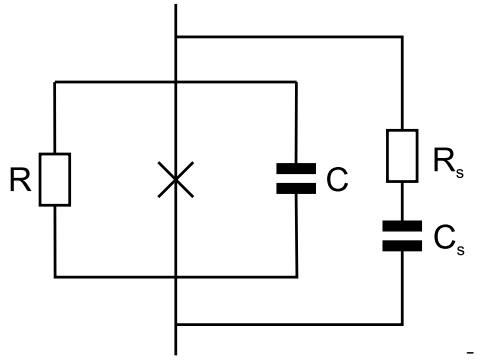

Figure 2: RSJ model with additional frequency dependent damping modeled by an external RC circuit.

$$\langle j_T(\tau) j_T(\tau')\rangle = 2\gamma\delta(\tau-\tau'), \qquad (4)$$

where $\tau = \omega_c t$, $j = J/J_c$, and $\omega_c = 2eRJ_c/\hbar$ is the characteristic frequency.

Here we introduce two main parameters:
(i) the McCumber parameter

$$\beta = \frac{\omega_c^2}{\omega_p^2} = \frac{2eR^2CJ_c}{\hbar}, \qquad (5)$$

where $\omega_p^2 = 2eJ_c/\hbar C$ is the Josephson plasma frequency;
(ii) the fluctuation parameter (normalized temperature)

$$\gamma = \frac{kT}{E_J} = \frac{2ekT}{\hbar J_c}. \qquad (6)$$

B. Extended RSJ model

As mentioned above, for the description of our experiments we need a frequency dependent damping which is achieved by the coupling to an external circuit as shown in Fig. 2. This model was already considered in detail by Kautz and Martinis[7] and is described by the following set of equations

$$\beta\frac{d^2\varphi}{d\tau^2} + \frac{d\varphi}{d\tau} + \alpha\left(\frac{d\varphi}{d\tau} - v\right) + \sin\varphi = j + j_T + j_{Ts}, \quad (7)$$

$$\beta\frac{dv}{d\tau} = \rho\left(\frac{d\varphi}{d\tau} - v - \frac{j_{Ts}}{\alpha}\right), \qquad (8)$$

where

$$\langle j_{Ts}(\tau) j_{Ts}(\tau')\rangle = 2\alpha\gamma\delta(\tau-\tau'). \qquad (9)$$

Here the parameters $\alpha = R/R_s$ and $\rho = \alpha C/C_s$ are introduced, $v(t)$ is the voltage across the external capacitance.

From the geometry of our samples we assume that C_s is the capacitance between the top and bottom contacts of the mesa and consequently $C_s \gg C$. The external

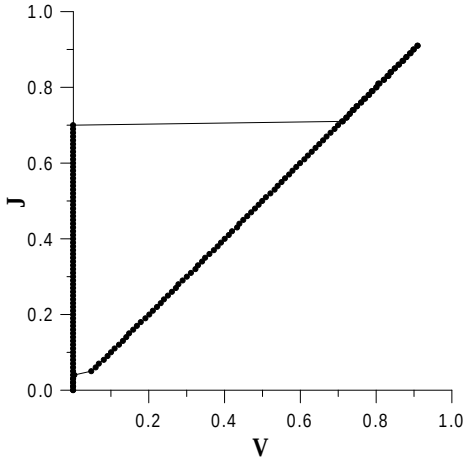

Figure 3: Typical current-voltage curves at low temperatures. The zero temperature critical current is suppressed by premature switching

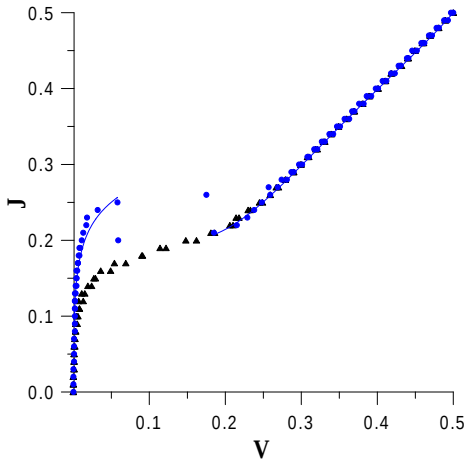

Figure 4: Typical current-voltage curves at intermediate temperatures with frequency-dependent damping (circles) and in the simple RSJ model (triangles).

resistance R_s is determined by a contact resistance and the resistance of the leads. For small mesas the single junction resistance R is very large, up to 10-100 kΩ and $R_s \ll R$ can be assumed. Therefore for small junctions the coupling to the external circuit should be included in the model calculations. In the classical fluctuation regime discussed in our paper it leads to the existence of a phase-diffusion branch instead of a zero-voltage superconducting branch.

Using this model as basis for numerical simulations we discuss in the following the typical behaviour of current-voltage curves in the different temperature regimes. In Section IV the model will be refined, in order to describe the experimental results in detail.

C. Premature switching at low temperatures ($T < T^*$).

At low temperatures a typical I-V curve as shown in Fig. 3 contains a superconducting branch (S-state) with zero voltage and a hysteretic jump to the resistive state (R-state). Due to fluctuations the critical (or, better to say switching) current J_s is random: the first strong enough thermal kick leads to a premature transition to the R-state, the probability of a back-transition to the S-state is very small. The average switching current $\langle J_s \rangle(T)$ depends on the sweeping velocity $\dot{I}$ of the current. It can be calculated numerically and analytically. We found that the results of our numerical simulations are in good agreement with the well known analytical result $\langle J_c \rangle(T)$ at low temperatures[15]

$$\langle J_s \rangle(T) = J_c(T) \left[1 - \left(\frac{\gamma}{2} \ln \frac{\omega_p \dot{I}}{2\pi I} \right)^{2/3} \right], \qquad (10)$$

Typically the logarithm is of the order of 10.

D. Phase diffusion branch at intermediate temperatures ($T \sim T^*$)

At intermediate temperatures the S-branch shows a bending with a finite voltage close to the switching current (see Fig. 4). As mentioned above this behaviour can be explained by phase diffusion within a model with frequency-dependent damping. Let us discuss briefly the properties of this model.

In the limit of zero frequency dissipation is determined by the junction resistance R alone, but at frequencies of the order of the plasma frequency ω_p due to the small impedance $1/\omega_p C_s$ of the external capacitance the dissipation is determined by the external resistance $R_s \ll R$ in parallel with R. Therefore for small junctions with $R_s \ll R$ dissipation at the plasma frequency is significantly larger then at zero frequency. For large-β hysteretic junctions it leads to the coexistence of a finite-voltage phase-diffusion S-branch and resistive branch. Thermal current-kicks stimulate jumps of the Josephson phase difference from one potential minimum to the next and therefore diffusion. On the other hand, the high dissipation at the plasma frequency – the characteristic frequency of these jumps, prevents from a fast transition to the resistive state with a running phase.

In Fig. 4 the phase diffusion branch in the model with frequency-dependent damping is shown (circles) together with the usual RSJ curve at similar parameters (triangles).

The phase diffusion branch can be found numerically, and has been observed in our experiments, only at intermediate temperatures. At low temperatures the voltage in the S-state is exponentially small. At high temperatures the usual phase diffusion takes place with a single-

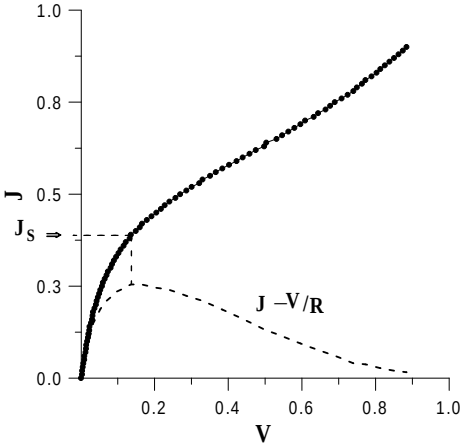

Figure 5: Typical current-voltage curves at high temperatures. The switching current J_s is determined as the current J for which the contribution of an average supercurrent (dashed line) is maximal

valued voltage-current curve.

E. Switching current at high temperatures ($T > T^*$).

At high temperatures the hysteresis disappears and only one single-valued I-V curve with a finite voltage at all currents exists (Fig. 5), but the average supercurrent, which is large at low voltages leads to a pronounced nonlinearity of I-V curve. We can extract approximately the contribution of the supercurrent to the I-V curve by subtracting the quasi-particle current, which in this model is a linear function of voltage. The current J at which the difference $J - V/R$ reaches its maximum (see Fig. 5) defines the switching current J_s. Note that this procedure to determine a switching current can also be applied at low temperatures and will be generally used later when experimental and theoretical results are presented and compared.

III. SAMPLE PREPARATION AND EXPERIMENTAL SET-UP

To measure the properties of ultrasmall intrinsic Josephson junctions we used a mesa geometry as sketched in Fig. 6. $Bi_2Sr_2CaCu_2O_{8+\delta}$ (BSCCO) single crystals and $Tl_2Ba_2CaCu_2O_{8+\delta}$ (TBCCO) thin films were used to prepare the samples[16]. Fig. 7 shows an SEM picture of a TBCCO sample. With our technique we were able to structure samples with lateral dimensions as small as $0.2 \times 0.2 \mu m^2$. The height of the mesas was between 60 Å and 1500 Å, which is equivalent to 4 - 100 intrinsic Josephson junctions.

Several small mesas with lateral dimensions of a few

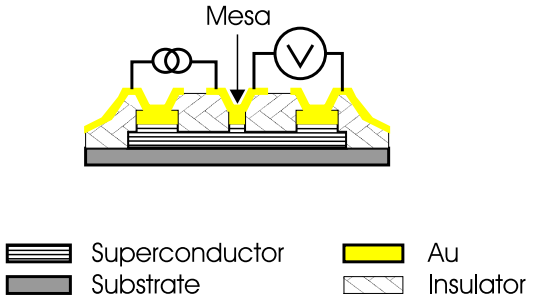

Figure 6: Sketch of the sample geometry

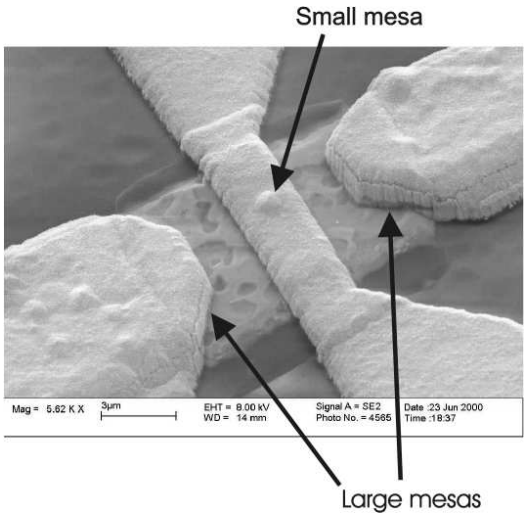

Figure 7: SEM picture of a TBCCO sample.

μm or lower were arranged on one chip. On the same chip also some larger mesas with lateral dimension of several μm were prepared. They serve as electrical contacts to the bulk superconductor. All mesas were contacted with Au leads. Current flows through one large mesa into the bulk superconductor and is extracted through the small mesa or vice versa. For voltage measurements one of the other large mesas is used. Due to the dimensions of the small mesa it was not possible to attach two isolated Au leads. Thus transport measurements were performed in a three-terminal configuration.

The Au electrode connected to the mesa leads to a suppression of the critical current and critical temperature of the uppermost intrinsic Josephson junction[17,18]. This degeneration might be explained by the assumption that the first superconducting layer is in close proximity with the normal Au electrode.

One sample was prepared in a step like geometry as proposed by Wang et al.[19]. Here we are able to record the I-V-characteristics in a true four-point geometry (sample s7n4 jj1 Table I).

The bias current was provided by a battery powered current source. The I-V-characteristics of the samples

sample	material	width (μm)	$J_s(4.3\,K)$ (μA)	T_c (K)	T^*_{exp} (K)
s5 jj3	TBCCO	0.7	16	103	65
CO-11-2-u-jjF	TBCCO	0.5	12.7	98.6	51
CO-11-2-u-jjD	TBCCO	0.5	5.75	97	32
usm9 jj8	BSCCO	0.4	0.74	86.5	12.5
r_el_2 jj 20	BSCCO	0.37	1.2	87.5	15
13 r	BSCCO	5	112	79.5	-
s7n4 jj1	BSCCO	2	40	90	-

Table I: Sample parameters. J_s is the switching current. T^*_{exp} is defined by the kink in the experimental J_s vs. T plots (see Fig. 9)

were recorded by applying dc currents and recording the voltages across mesas by digital voltmeters.

Measurements were done either in a standard helium dewar or in a magnet cryostat equipped with a 5 T Helmholtz solenoid. Temperatures could be varied between 4.2 K and room temperature. The temperature was measured with a platinum resistor for higher temperatures and a cernox resistor for low temperatures.

To reduce external noise low pass filters were used. In the helium dewar both cold filters and room temperature filters were used.

IV. EXPERIMENTAL RESULTS AND DISCUSSION

A. Experimental voltage-current curves and $J_s(T)$

We systematically measured voltage-current curves of mesas with different zero-temperature critical currents $J_c(0)$ at different temperatures (only a part of the sample parameters is presented in Table. I). Transition from high-hysteretic curves at low temperatures to phase-diffusion branches at crossover temperatures, and to a single resistive curve at high temperatures was clearly observed. Examples of experimental current-voltage curves at low (squares) and intermediate (filled circles) temperatures are shown in Fig. 8 (here the contact resistance is not subtracted). The well-known multibranch structure is observed.

The measurements of critical current were done mostly for the first (superconducting) branch, such that all junctions are in the S-state at low current and only one junction with the lowest critical current switches to the R-state. For this branch the average switching current J_s was determined. Its temperature dependence is shown in Fig. 9 for five samples with different values of $J_c(0)$ (open symbols) together with the results of the theoretical calculation (filled symbols, discussed in the next section). This picture is the main result of our work.

The main feature of all curves is a kink (or even minimum) in $J_s(T)$ at some temperature T^*_{exp}. This kink is

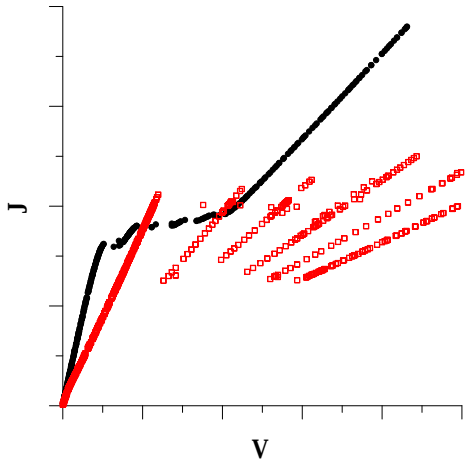

Figure 8: Typical experimental current-voltage curves at low (squares) and intermediate temperatures (circles).

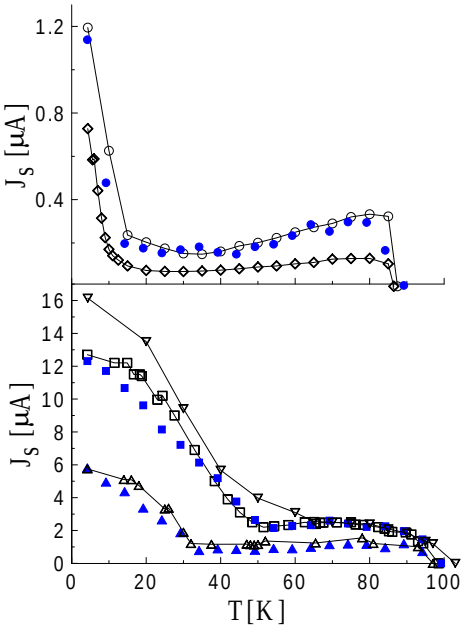

Figure 9: $J_s(T)$ for samples with different $J_c(0)$. Experiment (open symbols, the lines are guides to the eye), and theory (filled symbols).

absent in the $J_s(T)$ curves of mesas with large values of $J_c(0)$ and is shifted to lower temperatures with decreasing $J_c(0)$. T^*_{exp} corresponds approximately to the condition $E_J(T^*) = kT^*$, which strongly suggests thermal fluctuations as an origin of the observed features.

B. Theoretical voltage-current curves and $J_s(T)$

To describe the experimental result for the switching current $J_s(T)$ in detail it is necessary to take into account

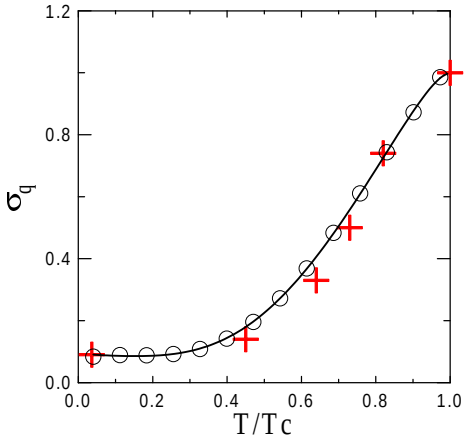

Figure 10: Quasiparticle conductivity of an intrinsic Josephson junction as function of T shown for incoherent tunneling and unitary intra-layer scattering (solid line), experimental points (crosses), and the fit g(T) used in further calculations (circles).

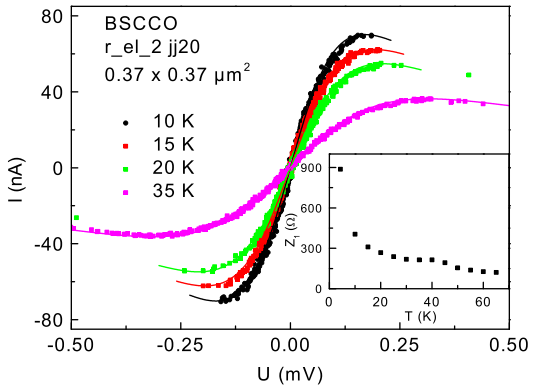

Figure 11: Phase-diffusion at low currents. Experimental points at different temperatures and fit to the analytical expression (11). The impedance Z_1 (shown in the insert) was used as a fitting parameter.

the temperature dependence of the parameters β and γ. These parameters are known functions of:

(i) the critical current $J_c(T)$ without fluctuations, which is determined (qualitatively also in HTSC) by the Ambegaokar-Baratoff relation.

(ii) the quasiparticle resistance $R(T)$, which we determined experimentally from current-voltage curves at small voltages (crosses in Fig. 10). We also calculated $R(T)$ at $V \to 0$ from microscopic theory for different models of interlayer tunneling (coherent and incoherent) and intra-layer scattering (Born and unitary). The best fit to the experimental results was obtained for incoherent tunneling in the unitary limit of intra-layer scattering with an elastic scattering frequency $\nu = 1$ meV. For the numerical simulations the function $g(T) = R(0)/R(T)$ is approximated by the fit (circles in Fig. 10).

The results of the theoretical calculations are presented in Fig. 9 for three different zero-temperature critical currents $J_c(0)$, the zero-temperature McCumber parameter $\beta(0)$ is in the range of 10^3 to 10^4. For each temperature we calculated $J_c(T)$, $\beta(T)$, $\gamma(T)$, and then produced current-voltage curves by numerical simulations starting from zero external current J. From these results the current J was determined, at which the average supercurrent $J_{sup} = J - V/R$ reaches its maximum. This current was defined previously as switching current J_s. The experimental switching currents J_s shown in Fig. 9 are defined in the same way. We find good agreement between experimental and theoretical curves. Also the current-voltage curves calculated at different temperatures show the same behaviour as the experimental curves.

From these results we conclude that the non-monotonic temperature dependence of $J_s(T)$ observed in experiment can well be explained by the model of large-β Josephson junction with thermal noise and coupling to an external impedance, if the proper temperature dependence of junction resistance is taken into account. In particular the strong suppression of J_s with temperature at low temperatures, $T < T^*$, is due to the premature switching effect in highly-hysteretic junctions. At high temperatures, $T > T^*$, the McCumber parameter β is smaller, the hysteresis disappears and the contribution of the average supercurrent to the current at finite voltages becomes larger, which leads to the plateau in the observed $J_s(T)$ dependence. Further discussions of the origins of non-monotonic temperature dependence of J_s can be found in the papers of Iansiti et al.[6] and Kautz and Martinis[7].

C. Phase-diffusion at low currents

For the junctions with the smallest critical current $J_c(0) \sim 1$ μA and highest quasiparticle resistance $R \gg R_s$ we investigated the low-current part of the current-voltage curves more precisely and found clear evidence of the phase-diffusion behaviour induced by the external circuit.

In the case $R_s \ll R$ and for $E_J < kT$ the phase-diffusion branch can be described by the analytical expression[15,20]

$$J(V) = \frac{4eTJ_s}{\hbar} \frac{Z_1 V}{V^2 + (2eZ_1T/\hbar)^2}, \qquad (11)$$

and the small finite resistance in the S-state at very low currents and at any temperature is given by[20]

$$R(J \to 0) = \frac{Z_1}{I_0^2(1/\gamma) - 1}, \qquad (12)$$

where $Z_1 \sim R_s$ is the impedance at low frequencies (of the order of the plasma frequency ω_p) and $I_0(x)$ is a Bessel function.

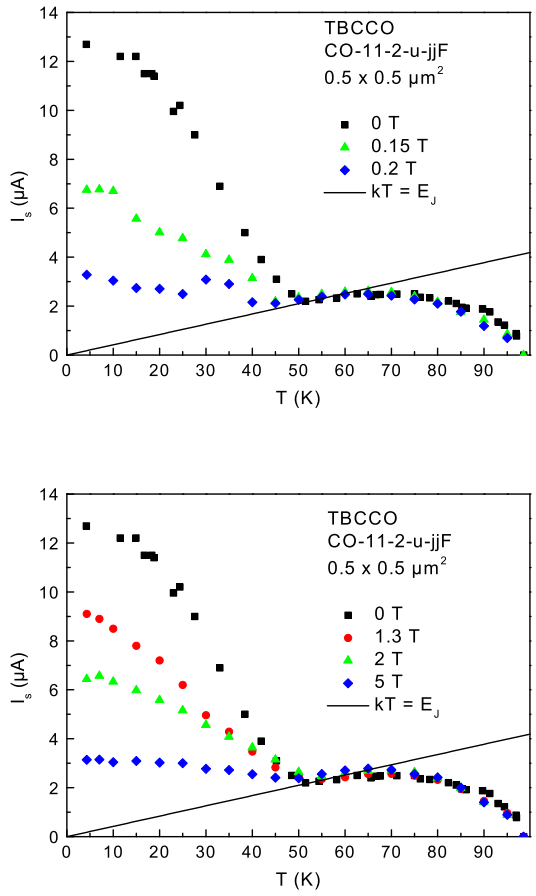

Figure 12: $J_s(T)$ at different perpendicular (upper figure) and parallel (lower figure) magnetic fields: experiment.

The experimental points presented in Fig. 11 can be fitted by Eq. (11). The best fitting result was achieved for a temperature dependent impedance Z_1 as shown in the insert. The origin of this temperature dependence is still unclear. It may be a contribution of the temperature dependent quasiparticle conductivity of other junctions in the mesa: when the temperature increases this conductivity also increases and the impedance decreases.

D. $J_s(T)$ in external magnetic field

Finally, we present here some results of measurements in an external magnetic field. Magnetic fields were applied by a 5 T superconducting split coil magnet. To measure $J_s(B)$ for parallel fields, the CuO_2-layers must be aligned with high precision parallel to the magnetic field. If the magnetic field has a component perpendicular to the layers pancake vortices enter the Josephson junctions and suppress the critical current. The orientation of samples in a magnetic field follows the procedure described in Ref. 21. The junction is biased at a fixed current and a fixed magnetic field is applied. Then the voltage change is monitored while the angle φ between the external field and the CuO_2-layers was varied with a precision rotation stage. When measured at high enough temperatures the field-induced changes of the I-V-characteristic were reversible and could be used for alignment. Thus, the field orientation relative to the CuO_2-layers could be adjusted to an accuracy of 0.01°.

The main and most general experimental result is presented in Fig. 12. In both perpendicular and parallel magnetic fields $J_s(T)$ *is not changed for* $T > T^*$, while for $T < T^*$ one finds a field dependent suppression of $J_s(T)$.

To understand this behaviour qualitatively, we explore the well-known sin-Gordon equation, which describes long Josephson junctions (see Ref. 22,23)

$$\beta\frac{\partial^2\varphi}{d\tau^2}-\frac{\partial^2\varphi}{dx^2}+\frac{\partial\varphi}{d\tau}+\sin(\varphi+B_\parallel x+\delta\varphi(x,\tau))=j+j_T(x,\tau). \tag{13}$$

Here the coordinate x is in units of the Josephson length λ_J, $B_\parallel$ is the component of the external magnetic field parallel to the layers, and $\delta\varphi(x,\tau)$ is a random phase distribution produced by pancake-vortices in perpendicular magnetic field[24,25,26]. We include the phase variation due to the external magnetic field in the *sin*-function instead of using the more familiar procedure, where the magnetic field is taken into account by boundary conditions (both methods are equivalent). The random functions $j_T(x,\tau)$ and $\delta\varphi(x,\tau)$ describing noise are assumed to be Gaussian and δ-correlated in space

$$\langle j_T(x,\tau)j_T(x,\tau')\rangle = 2\gamma\delta(\tau-\tau')\delta(x-x'), \tag{14}$$

$$\langle\delta\varphi(x,\tau)\delta\varphi(x,\tau')\rangle \propto B_z\delta(x-x'). \tag{15}$$

In the last expression we accept a linear magnetic field dependence of the correlation function and neglect the time-dependence of phase shifts assuming that the pancakes are frozen or move slowly enough. In a more realistic approach the space and time dependence of correlation functions of the pancake disorder depend on a state of the vortex matter, is it liquid, glass-like, or solid.

Results of our numerical simulations with magnetic field are presented in Fig. 13 for several values of perpendicular and parallel fields. The main result of our calculations (as well as similar experimental results) is the sensitivity to a magnetic field at low temperatures and the absence of considerable influence at high temperatures.

Qualitatively this result can be understood in the following way. The main effect of the magnetic field is to produce phase shifts, regular for the parallel field and random for the perpendicular field. At low temperatures, when J_s is determined by the premature switching mechanism, the reduction of J_c in the magnetic field is important because the energy barrier becomes smaller.

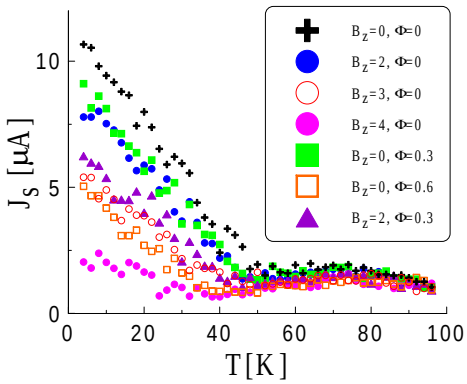

Figure 13: $J_s(T)$ at different perpendicular (circles), parallel (squares), and oblique (triangles) magnetic fields: theory. Φ is the magnetic flux of the parallel field through a Josephson junction in units of the flux quantum Φ_0.

But in the high-temperature regime where phase diffusion is strong, additional phase shifts $\delta\varphi(x,\tau)$ produced by the magnetic field cannot compete with the existing large thermal phase fluctuations.

V. SUMMARY

In this paper we discuss new experiments on the influence of thermal noise on current-voltage curves and the switching current of small area intrinsic Josephson junctions. Two main effects of thermal fluctuations: premature switching and phase-diffusion, are observed. The non-monotonic temperature dependence of the switching current is explained theoretically with a help of an extended RSJ model (including thermal noise and a frequency dependent external impedance) taking into account the proper temperature dependence of parameters. The different behaviour of the switching current at low and high temperatures in the presence of magnetic fields can be explained in a similar way.

Acknowledgements

We thank G. Blatter and L.N. Bulaevskii for valuable discussions.

This work was supported by the German Science Foundation (D.R.), and by the Swiss National Center of Competence in Research "Materials with Novel Electronic Properties-MaNEP" (C.H.).

[1] R. Kleiner, F. Steinmeyer, G. Kunkel, and P. Müller, Phys. Rev. Lett. **68**(15), 2394 (1992).
[2] R. Kleiner and P. Müller, Phys. Rev. B **49**(2), 1327 (1994).
[3] P. Müller, in *Festkörperprobleme/Advances in Solid State Physics*, edited by R. Helbig (Vieweg, Braunschweig, 1994), vol. 34, p. 1.
[4] A. A. Yurgens, Superconductor Science and Technology **13**(8), R85 (2000).
[5] T. A. Fulton and L. N. Dunkleberger, Phys. Rev. B **9**(11), 4760 (1974).
[6] M. Iansiti, M. Tinkham, A. Johnson, W. Smith, and C. Lobb, Phys. Rev. B **39**(10), 6465 (1989).
[7] R. L. Kautz and J. M. Martinis, Phys. Rev. B **42**(16), 9903 (1990).
[8] S. Martin, E. S. Hellman, A. Kussmaul, and E. H. Hartford, Jr., Phys. Rev. B **48**(9), 6626 (1993).
[9] L. I. Glazman and A. E. Koshelev, Phys. Rev. B **43**(4), 2835 (1991).
[10] G. Blatter, M. V. Feigel'man, V. B. Geshkenbein, A. I. Larkin, and V. M. Vinokur, Rev. Mod. Phys. **66**(4), 1125 (1994).
[11] L. N. Bulaevskii, V. L. Pokrovsky, and M. P. Maley, Phys. Rev. B **76**(10), 1719 (1996).
[12] A. E. Koshelev, Phys. Rev. Lett. **77**(18), 3901 (1996).
[13] A. E. Koshelev and L. N. Bulaevskii, Phys. Rev. B **60**(6), R3743 (1999).
[14] P. A. Warburton, A. R. Kuzhakhmetov, G. Burnell, M. G. Blamire, and H. Schneidewind, Phys. Rev. B **67**, 184513 (2003).
[15] M. Tinkham, *Introduction to Superconductivity* (McGraw-Hill, New York, 1996), 2nd ed.
[16] Y. Koval, A. Franz, P. Müller, and H. Schneidewind, *Preparation and characterization of submicron stacked Josephson junctions on Tl-2212 epitaxial films* (2000), EURESCO conference 2000-147: Future Perspectives of Superconducting Josephson Devices, Maratea 2000.
[17] N. Kim, Y. J. Doh, H.-S. Chang, and H.-J. Lee, Phys. Rev. B **59**(22), 14 639 (1999).
[18] S. Rother, Y. Koval, P. Müller, R. Kleiner, D. A. Ryndyk, J. Keller, and C. Helm, Phys. Rev. B **67**(2), 024510 (2003).
[19] H. B. Wang, P. H. Wu, and T. Yamashita, Phys. Rev. Lett. **87**(10), 107002 (2001).
[20] G.-L. Ingold, H. Grabert, and U. Eberhardt, Phys. Rev. B **50**(1), 395 (1994).
[21] A. Irie, S. Heim, S. Schromm, M. Mößle, T. Nachtrab, M. Gódo, R. Kleiner, P. Müller, and G. Oya, Phys. Rev. B **62**(10), 6681 (2000).
[22] A. Barone and G. Paterno, *Physics and applications of the Josephson effect* (Wiley, New York, 1982).
[23] K. Likharev, *Dynamics of Josephson junctions and circuits* (Gordon and Breach, Amsterdam, 1996).
[24] L. Bulaevskii, D. Dominguez, M. Maley, A. Bishop, O. K. Tsui, and N. Ong, Phys. Rev. B **54**(10), 7521 (1996).
[25] L. N. Bulaevskii, D. Dominguez, M. P. Maley, and A. R. Bishop, Phys. Rev. B **55**(13), 8482 (1997).
[26] A. E. Koshelev, L. N. Bulaevskii, and M. Maley, Phys. Rev. B **62**(21), 14403 (2000).